ANNALI DI GEOFISICA, VOL. XXXVI, N. 5-6, September-October 1993

A numerical experiment on the spherical harmonic analysis of core and crustal geomagnetic fields

Bejo Duka
Faculty of Natural Sciences, Department of Physics, University of Tirana, Albania

Abstract
Different quadrature methods in the spherical harmonic analysis of the geomagnetic field are compared. For high degree and order coefficient calculations, the Gauss-Legendre quadrature has been found to be the best method. The feasibility of this method has been tested here firstly on simulated global field values from DGRF80. Then, using this quadrature, the spherical harmonic coefficients up to degree n=134 for the magnetic field of a simulated crustal model are calculated. Some interesting results in the behaviour of spherical harmonic coefficients are considered.

Key words *spherical harmonics – geomagnetic spectrum*

1. Introduction

The geomagnetic field between the Earth's surface and the ionosphere can be considered to be curl-free. This allows the representation of magnetic induction $\boldsymbol{B}$ as the gradient of a scalar potential V, which satisfies the Laplace equation. In spherical coordinates (r, θ, ϕ) the general solution of Laplace equation is the infinite series of spherical harmonics of degree n and order m multiplied by a radial function. In the case of internal geomagnetic field it is given by:

$$V = a \sum_{n=1}^{\infty} \sum_{m=0}^{n} (a/r)^{n+1} (G_n^m \cos m\phi + H_n^m \sin m\phi) P_n^m(\cos\theta) \qquad (1.1)$$

where a is a reference radius of the Earth (usually the mean radius 6371.2 km), r is the radial distance from the centre of the Earth, ϕ and θ represent longitude and colatitude, respectively.

The objective of spherical harmonic analysis (SHA) is to compute the spherical harmonic coefficients (SHC) G_n^m, H_n^m from a given set of observed field data.

SHA of the geomagnetic field is usually done by using the method of least squares (LS) in conjunction with a truncated spherical harmonic series up to a prefixed maximum value of degree and order. It has been used by many authors and refined in different ways either in the global case (Schmitz and Cain, 1983; Whaler and Gubbins, 1981) or in the regional case (De Santis, 1991; Haines, 1985). Due to the enormous computer memory requirement, LS method cannot be used for computation of high degree and order coefficients (above n=30). For the calculation of such coefficients the integration methods that exploit the orthogonality properties of spherical harmonics are used (Alldredge and Kawasaki, 1981; Cain *et al.*, 1989, 1990; Kawasaki *et al.*, 1989; Schmitz *et al.*, 1989). Quinn and Barrick (1987) have used the Fast Fourier Transform (FFT) for the spherical harmonic modelling of the geomagnetic field up to degree n=12, generating the data from WC-geomagnetic model. Judging from the intrinsic

speed of FFT method (a few seconds for n=12) and the small errors (differences between the input coefficients of WC-model and calculated by FFT coefficients) one would expect to use this method for the high degree and order coefficient calculation. But the FFT technique requires a set of data strictly arranged in an equiangular grid covering the entire surface of a sphere and an extension of the grid in colatitude direction to the interval $(-\pi, \pi)$. Such extention is described by Quinn and Barrick (1987) but it is valid only when the data are represented as a finite sum of spherical harmonic terms (so it is more suitable for core field modelling).

In some other methods the Fourier analysis in longitude and least squares in latitude or different quadratures in latitude are used. Seeing that the calculation results are mostly influenced by the integration in latitude we have tested here different ways of such integration on data simulated from a global model. Deducing that the best way is the Gauss-Legendre quadrature, we have used it also for the SHA of a modelled crustal geomagnetic field. The purpose of this latter analysis was to see the behaviour of SHC at high degrees and orders.

2. Different ways of integration for the SHC computation

When the radial component B_r of the field is known on the sphere surface (of radius a), taking advantage of the orthogonality properties of spherical harmonics, the SHC can be recovered by integration on the sphere surface (Schmitz *et al.*, 1989):

$$\begin{Bmatrix} G_n^m \\ H_n^m \end{Bmatrix} = \{(2n+1)/[4\pi(n+1)]\}(r/a)^{n+2} \int_0^{2\pi}\int_0^{\pi} B_r(r,\ \theta,\ \phi)P_n^m(\cos\theta)\cdot \begin{Bmatrix} \cos m\phi \\ \sin m\phi \end{Bmatrix} \sin\theta d\theta d\phi \quad (2.1)$$

In practice, the double integral can be evaluated in two stages, first the part in ϕ:

$$\begin{Bmatrix} A_m(\theta) \\ B_m(\theta) \end{Bmatrix} = (1/\delta_m\pi) \int_0^{2\pi} B_r(r,\ \theta,\ \phi) \begin{Bmatrix} \cos m\phi \\ \sin m\phi \end{Bmatrix} d\phi \quad (m = 0,\ 1,\ 2,...) \quad (2.2)$$

(where $\delta_m = 2$ for m=0 and $\delta_m = 1$ for $m>0$), then followed by the part in θ:

$$\begin{Bmatrix} G_n^m \\ H_n^m \end{Bmatrix} = \delta_m[(2n+1)/4(n+1)](r/a)^{n+2} \int_0^{\pi} \begin{Bmatrix} A_m(\theta) \\ B_m(\theta) \end{Bmatrix} P_n^m(\cos\theta)\sin\theta d\theta \quad (2.3)$$

In the following calculation, for numerically evaluating the first integral, the extended trapezoidal rule (*e.g.* Abramowitz and Stegun, 1972) has always been used. For evaluating the second integral, the above quadrature method and the Gauss-Legendre quadrature have been used and compared. B_r data will be simulated by DGRF80 (the definitive geomagnetic reference field at 1980.0; Barraclough, 1987) on appropriate grids with maximum degree n=10.

2.1. *Trapezoidal quadrature on equal longitude and latitude spaced data*

In this case both integrals are numerically evaluated by the same quadrature (trapezoidal) method at r=a:

$$\begin{Bmatrix} G_n^m \\ H_n^m \end{Bmatrix} = \{(2n+1)/[4\pi(n+1)]\} \sum_{i=1}^{N_1}\sum_{j=1}^{N_2} B_r(\theta_i,\phi_j)P_n^m(\cos\theta_i)\cdot \begin{Bmatrix} \cos m\phi_j \\ \sin m\phi_j \end{Bmatrix} \sin\theta_i\Delta\theta_i\Delta\phi_j \quad (2.4)$$

where $\Delta\theta_i = \pi/N_1$, $\Delta\phi_j = \pi/N_2$, $\theta_i = i\pi/N_1$, $\phi_j = j\pi/N_2$.

Generally the greater the numbers of intervals N_1, N_2, the more accurate the SHC will be. We have tested several θ and ϕ divisions and we have stopped at a reasonable division: $\Delta\theta_i = \pi/100$, $\Delta\phi_j = 2\pi/400$, ($N_1 = 100$, $N_2 = 400$, number of data points 40 000). With this procedure, the computation of Gauss coefficients from (2.4) gives a r.m.s. deviation: 1.66 nT.

In fig. 1a the differences between the input coefficients (DGRF80 coefficients) and computed coefficients are shown. For the numbering of coefficients in x-axis the notation (Whaler and Gubbins, 1981):

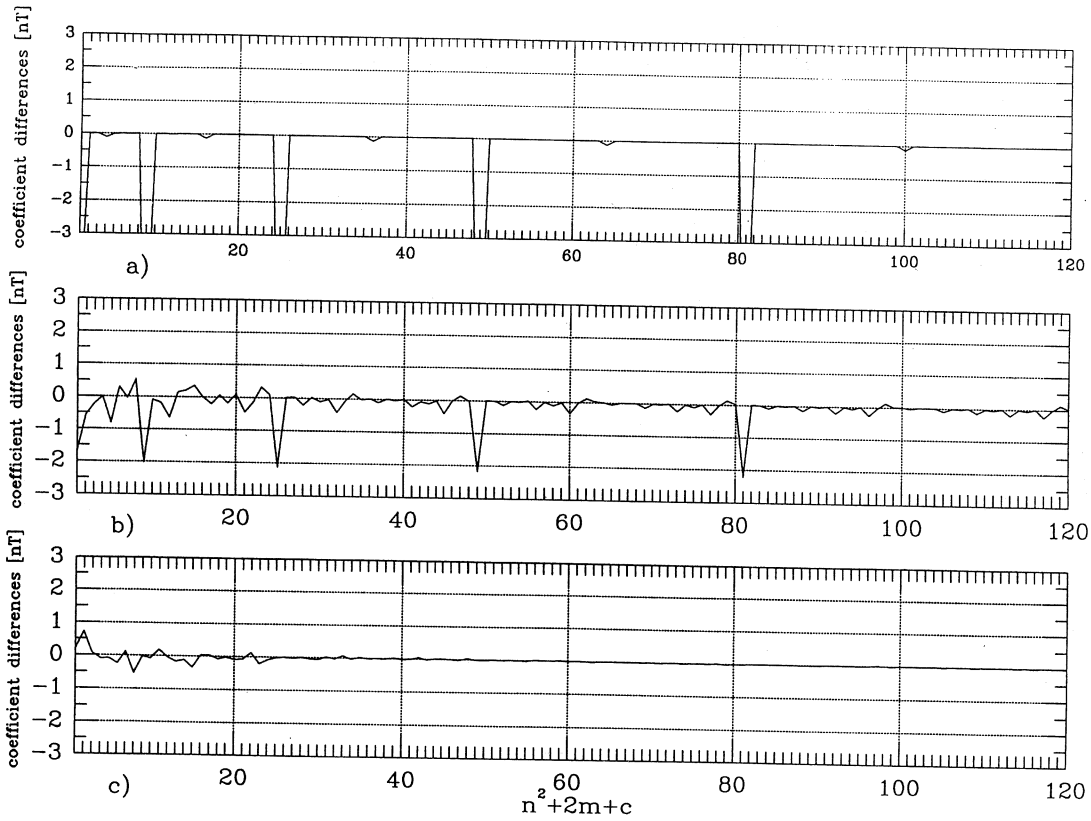

Fig. 1. Differences between known input coefficients and coefficients computed by: a) trapezoidal quadrature on equal longitude and latitude spaced data; b) trapezoidal quadrature on equal subsurface division; c) Gauss-Legendre quadrature, depending on degree and order of coefficients.

$\beta = n^2 + 2m + c$, where

$$c = \begin{cases} -1 & \text{for } G_n^m \ m\#0 \\ 0 & \text{for } H_n^m \text{ and } G_n^0 \end{cases}$$

is used.

It can be seen that the differences are usually smaller than 0.2 nT, except some values: $G_1^0\,(\beta = 1)$, $G_3^0\,(\beta = 8)$, $G_5^0\,(\beta = 24)$ etc., generally for G_{2n+1}^0 (n=0,1,2,3..); *i.e* for zero order and odd degrees.

In this specific case the data points are denser near the poles ($\theta = 0$, $\theta = \pi$) than along the equator. Dealing with a surface integral on the sphere, an equal subsurface division on the sphere should be better for the numerical approximation (Schmitz and Cain, 1983).

2.2. *Trapezoidal quadrature on equal subsurface division*

The integrals are computed by the same algorithm (2.1) on synthesized data with a uniform division of θ values: $\Delta\theta = \pi/N_1$ but with a variable division of ϕ values according to θ_i values:

$$\Delta\phi_i = 2\pi/N_{2,i} \qquad (2.5)$$

where $N_{2,i}$ (the number of divisions in ϕ) is the integer part of $2N_1 \sin\theta_i$. It follows that we have nearly the same subsurface on the sphere:

$$\Delta S_i = \sin\theta_i \Delta\theta \Delta\phi_i \simeq (\pi/N_1)^2 \qquad (2.6)$$

Figure 1b shows the corresponding differences between input coefficients (DGRF80 coefficients) and computed coefficients for $N_1 = 200$ and 50 834 data points. As it can be seen the new differences are a little smaller than in the previous case (fig. 1b) for odd degrees (m=0) but a little greater for all other degrees and orders. However, the overall r.m.s. deviation was now smaller: 0.45 nT.

The biggest errors in the computation of odd degree n and order m=0 coefficients by trapezoidal and other quadrature were already mentioned by Schmitz *et al.* (1989) (they found biggest errors for those coefficients with m=0 or 1 and with degree n of the same parity as the largest coefficient in the input coefficient set) and were attributed to «numerical inexactness (referring to polynomials)» of such quadratures. We think that, in our case, this can be explained by the different accuracy of equal spaced numerical integration (in θ) for different parity of the integrated function which is in the form (2.3), *i.e.* $A_m(\theta)P_n^m(\cos\theta)\sin\theta$ for equal longitude latitude spaced division and $A_m(\theta)P_n^m(\cos\theta)$ for equal subsurface division. The term $\sin\theta$ has even parity in the integration interval $(0, \pi)$, so it does not influence the parity of the integrated function. For m=0 the function $A_0(\theta) = \langle B_r(\theta, \phi)\rangle_\phi$, for which the most important term is the dipolar term, depends upon θ as cos θ and we can consider it as an odd function. The parity of P_n^0 is determined by the parity of n. So, when n is odd the integrated function is even, otherwise the integrated function is odd, as it can be seen in fig. 2 (this figure shows two exam-

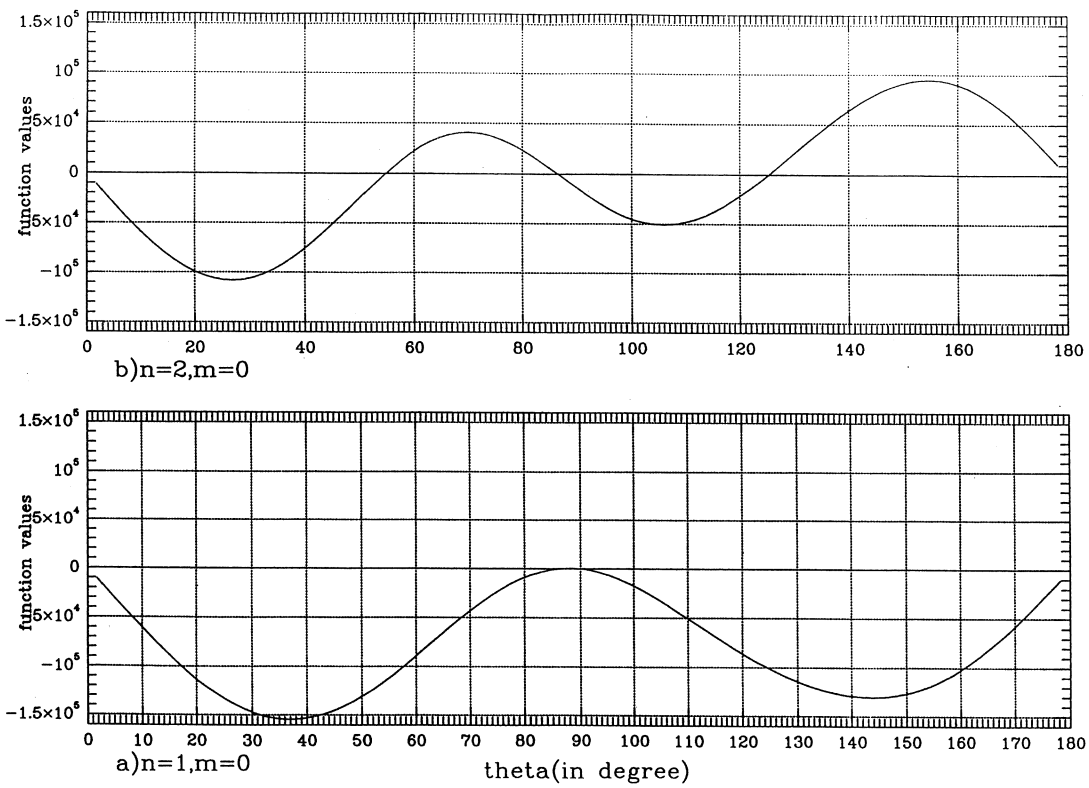

Fig. 2. The graphics of integrated functions depending on colatitude.

ples of $A_m(\theta)P_n^m(\cos\theta)$ function: the upper graphic is for the case of n=2, m=0 and the lower graphic is for the case of n=1, m=0). For odd functions (as the upper curve of fig. 2) the integration errors tend to compensate each other in two half-intervals (0, $\pi/2$) and ($\pi/2$, π) while for even functions (lower graphic of fig. 2) they tend to add in two half-intervals.

2.3. *Gauss-Legendre quadrature*

The first integral is again evaluated by the same trapezoidal rule (the same number of $\Delta\phi$ interval $N_2 = 400$ for each value of θ), while the second integral is evaluated by using the Gauss-Legendre quadrature formula (*e.g.* Abramowitz and Stegun, 1972):

$$\int_0^{\pi} f(\theta)d\theta = \sum_{i=1}^{N} f(\theta_i)\omega_i \qquad (2.7)$$

where the colatitudes θ_i are the roots of Legendre polynomial of degree N, the weights ω_i are chosen so as to make quadrature exact whenever $f(\theta)$ is a polynomial of degree less or equal to 2N-1. Here we have used the algorithm given by Press *et al.* (1987) for the generation of θ_i and ω_i, which were the same as those tabulated by Abramowitz and Stegun (1972).

The differences between input and calculated coefficients (N=96, data points 38 400) are shown in fig. 1c. As it can be seen, such differences are smaller than 0.5 nT (apart from the second coefficient) and tend to be zero for high degree and order.

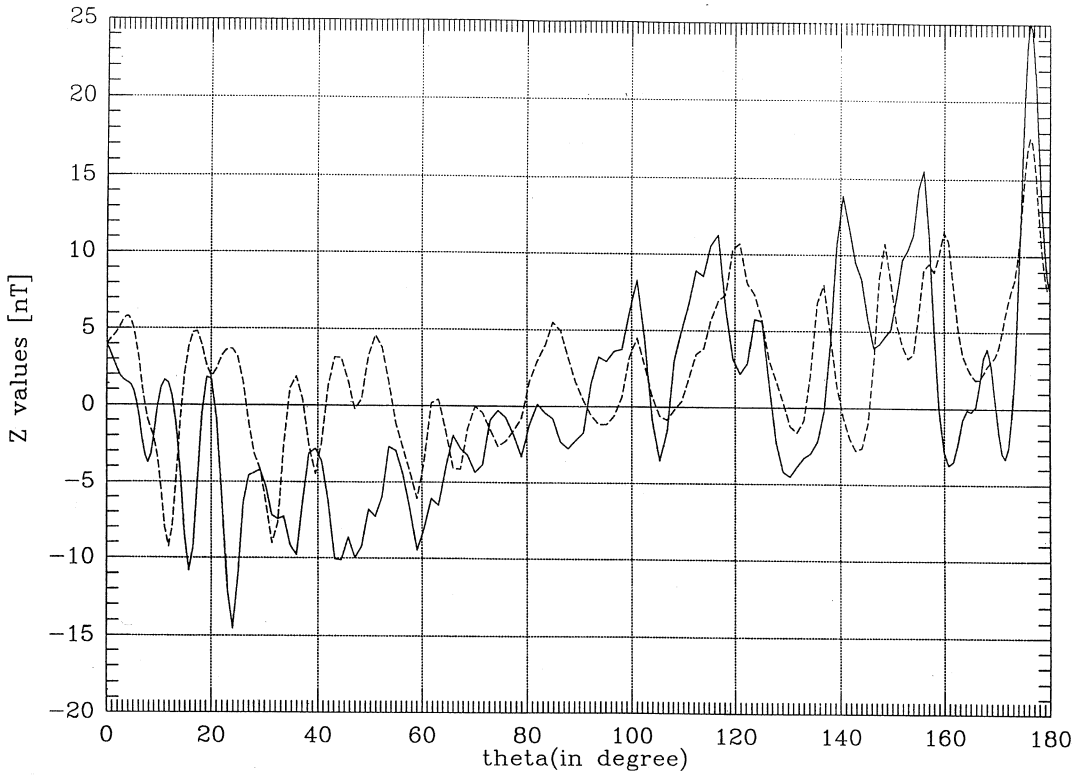

Fig. 3. The graphics of crustal field values along meridians ϕ=0 and ϕ=180 vs colatitude.

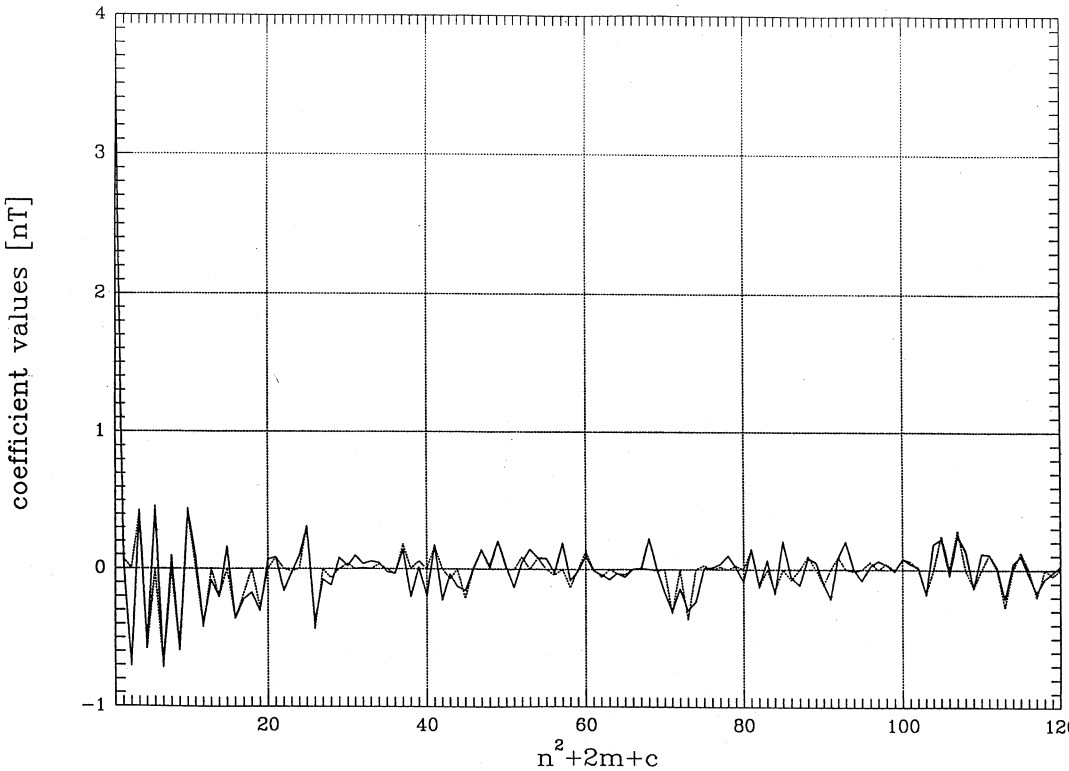

Fig. 4. The SHC calculated by Gauss-Legendre quadrature and true SHC computed by Hurwitz formulas from degree n=1 up to degree n=10.

The found r.m.s. deviation was definitively better than previous quadratures: 0.10 nT.

3. SHA of a modeled crustal geomagnetic field

The above analysis shows that the most accurate way to compute SHC by integration is the Gauss-Legendre quadrature method. It can be successfully applied even when a fewer global data are taken. The only disadvantage is that it requires data taken from determined points (θ_i must be a root of Legendre polynomials), which is difficult to realize in practice (obviously true data are mostly sparsely distributed on the sphere without any relation with Legendre polynomial zeros in colatitude).

Then we have used the Gauss-Legendre quadrature for SHA of a geomagnetic field similar to that originated in the crust. For the simulation of such a field, we constructed a global model of the Earth's crust similar to that of Meyer *et al.* (1983). We did not aim at constructing a truly realistic model of the whole Earth's crust, but to acquire a data distribution like the crustal geomagnetic field. We chose a simple crustal model composed of one-layer spherical blocks with the same thickness (30 km) and the same volume τ of that of a spherical block of $4^\circ \times 4^\circ$ at the Equator. Considering only induced magnetization, for the calculation of the magnetic field, each block was substituted by a single dipole placed at the center of the block (2548 dipoles in total at the same depth of 15 km) and directed parallelly to the DGRF80 in that place.

The magnetic moment of i^{th} block is:

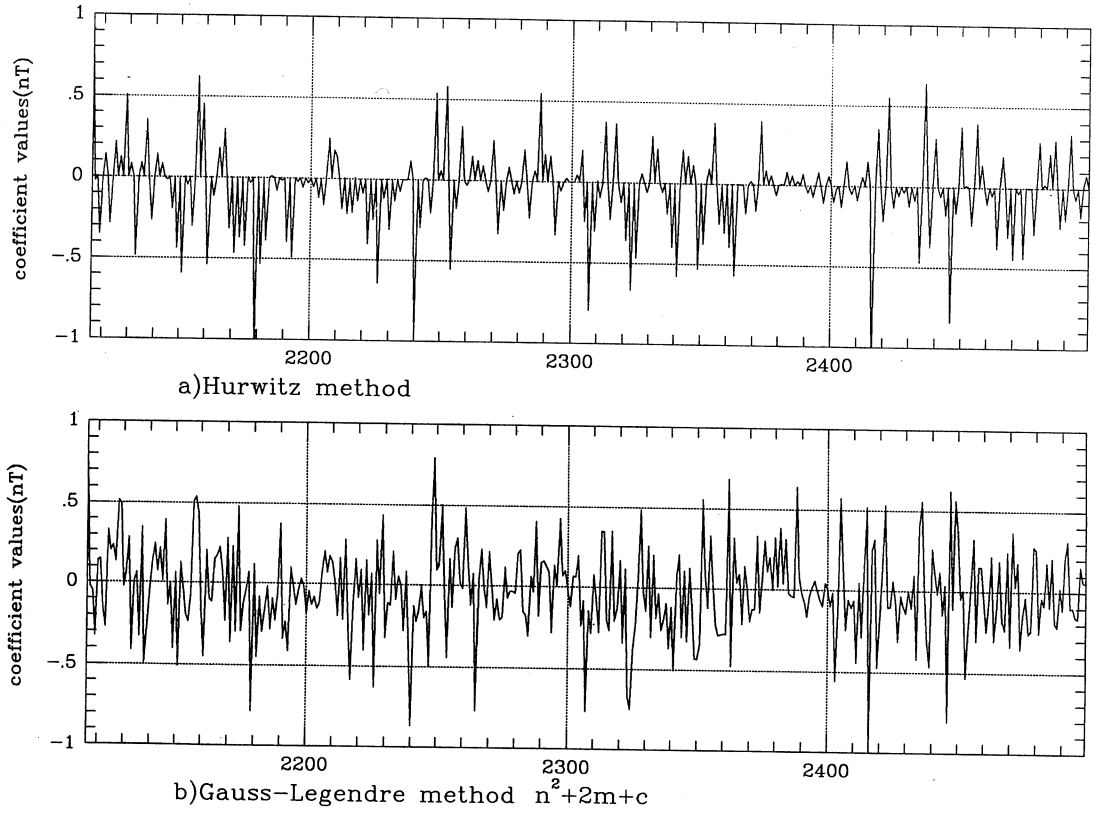

Fig. 5. The SHC calculated by Gauss-Legendre quadrature and true SHC from degree n=46 up to degree n=49.

$$\boldsymbol{m}_i(r_i, \theta_i, \phi_i) = \chi_i \tau \boldsymbol{F}_i \tag{3.1}$$

where $\boldsymbol{F}_i$ is the total intensity field of DGRF80 at the block centre $P_i(r_i, \theta_i, \phi_i)$, χ_i is the susceptibility of i^{th} block. The susceptibilities of blocks are selected from a ten values table (Meyer *et al.*, 1983) by a random procedure. The spherical components of dipole moment are calculated by DGRF80 elements (inclination I, declination D) at the corresponding point P_i:

$$\begin{aligned} m_{r_i} &= -m_i \sin I_i \\ m_{\theta_i} &= -m_i \cos I_i \cos D_i \\ m_{\phi_i} &= m_i \cos I_i \sin D_i \end{aligned} \tag{3.2}$$

The contribution to the potential of the magnetic induction $\boldsymbol{B}$ from the i^{th} dipole calculated to a fixed external point $P(r, \theta, \phi)$ is (in SI formulation):

$$V_i(r, \theta, \phi) = (\mu_0/4\pi)\boldsymbol{m}_i \cdot \boldsymbol{l}_i / l_i^3 \tag{3.3}$$

where $\boldsymbol{l}_i$ is the vector distance between the dipole position P_i and the point P. Expressing the direction cosines between the spherical components m_{r_i}, m_{θ_i}, m_{ϕ_i} and the vector $\boldsymbol{l}_i$ by the known coordinates of $\boldsymbol{m}$, P, P_i we can find:

$$V_i = (\mu_0/4\pi)[m_{r_i}(ra_i - r_i) - m_{\theta_i} r b_i + m_{\phi_i} r c_i]/l_i^3 \tag{3.4}$$

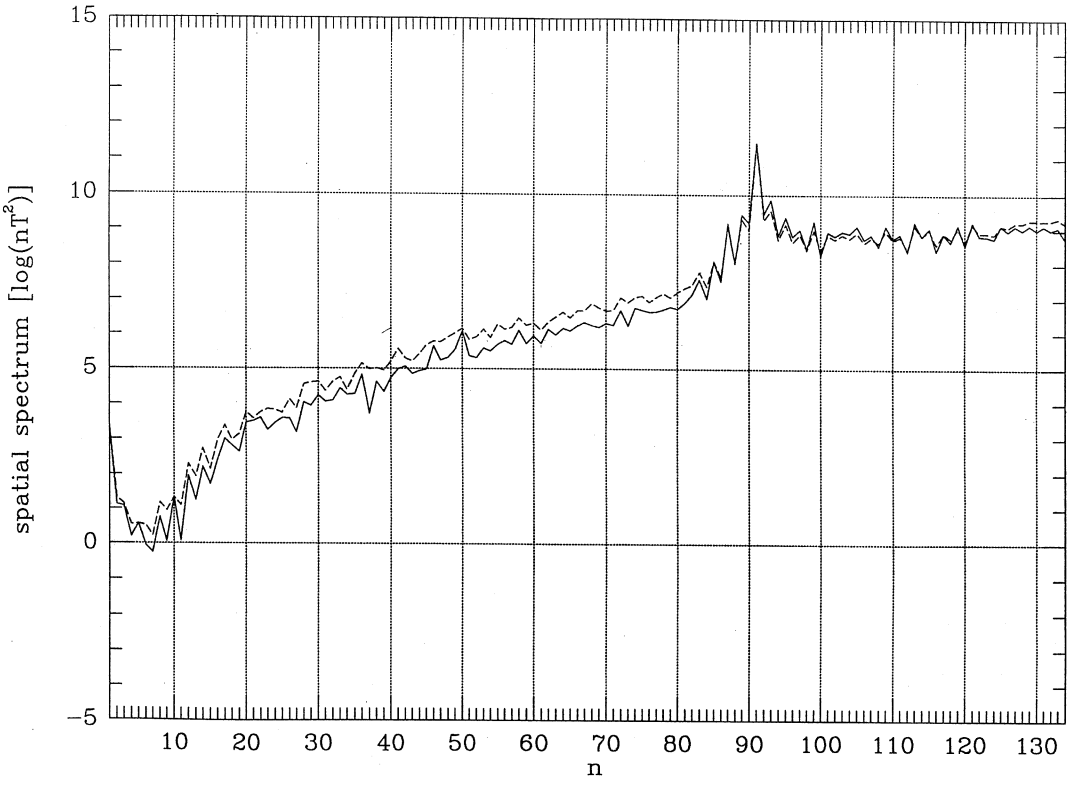

Fig. 6. The power spatial spectrum (at the reference radius of 6371.2 km) depending on degree n.

where:

$$
\begin{aligned}
l_i &= \sqrt{r^2 + r_i^2 - 2rr_ia_i} \\
a_i &= \cos\theta\cos\theta_i + \sin\theta\sin\theta_i\cos(\phi - \phi_i) \\
b_i &= \cos\theta\sin\theta_i - \sin\theta\cos\theta_i\cos(\phi - \phi_i) \\
c_i &= \sin\theta\sin(\phi - \phi_i) \qquad (3.5)
\end{aligned}
$$

The vertical component of the field ($Z_i = -B_{r,i} = \partial V_i/\partial r$) is:

$$
\begin{aligned}
Z_i = (\mu_0/4\pi)\{&m_{r_i}[a_i(1/l^3 + 3r(r_ia_i - r)/l_i^5) - 3r_i \\
&(r_ia_i - r)/l_i^5] + m_{\theta_i}[-b_i(1/l_i^3 + 3r(r_ia_i - r)/l_i^5)] \\
&+ m_{\phi_i}[c_i(1/l_i^3 + 3r(r_ia_i - r)/l_i^5)]\} \qquad (3.6)
\end{aligned}
$$

Summing up for contributes of all dipoles we have calculated the Z component of crust model field for r=6371.2 + h (for a possible satellite survey h=450 km was chosen) at grid points appropriate for Gauss-Legendre algorithm. The behaviour of Z along the meridians $\phi = 0$ (dashed graphic) and $\phi = 180^\circ$ (solid graphic) from such a synthetic model is shown in fig. 3.

In order to estimate the accuracy of SHC calculation of the crustal field, we have compared the SHC values calculated by the Gauss-Legendre algorithm with the exact values calculated analytically. For an internal eccentric dipole distant r_i from the center of a spherical Earth of radius a (r_i<a), in colatitude θ_i and longitude ϕ_i, it may be shown that the SHC of its external field are given by the sum of three sets of coefficients (Hurwitz, 1960):

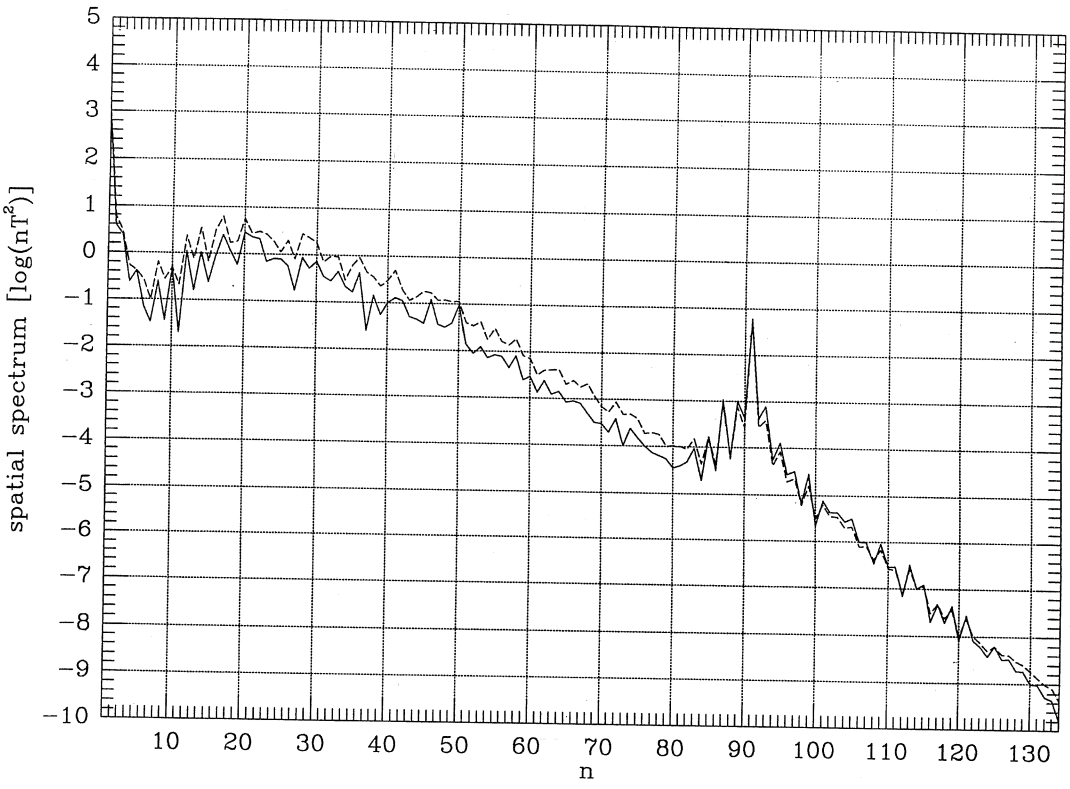

Fig. 7. The power spatial spectrum (at the reference radius of 6821.2 km) depending on degree n.

$$
\begin{aligned}
G_n^m(1,i) &= (m_{r_i}/a^3)(r_i/a)^{n-1} n P_n^m(\cos\theta_i)\cos(m\phi_i) \\
H_n^m(1,i) &= G_n^m(1,i)\mathrm{tg}(m\phi_i) \\
G_n^m(2,i) &= (m_{\theta_i}/a^3)(r_i/a)^{n-1} dP_n^m(\cos\theta_i)/d\theta\cos(m\phi_i) \\
H_n^m(2,i) &= G_n^m(2,i)\mathrm{tg}(m\phi_i) \\
G_n^m(3,i) &= -(m_{\phi_i}/a^3)(r_i/a)^{n-1} m P_n^m(\cos\theta_i)\sin(m\phi_i)/\sin(\theta_i) \\
H_n^m(3,i) &= -G_n^m(3,i)\mathrm{ctg}(m\phi_i) \qquad (3.7)
\end{aligned}
$$

Summing up for all our eccentric dipoles, we found the exact values of SHC of our crustal model field. Such values are referred below as true SHC (because calculated with the direct formulas (3.7) by Hurwitz).

Since it is impossible to represent all coefficient values of the modelled crustal we have shown some of them: in fig. 4 for degree from n=1 to n=10 (the dashed graphic is for Gauss-Legendre quadrature and the other graphic shows the true SHC); in fig. 5 for degree from n=46 to n=49 (the upper graphic a) is for Hurwitz's method, while the lower graphic is for Gauss-Legendre quadrature). It can be seen that both graphics have the same going and the differences between the exact values of coefficients and calculated by Gauss-Legendre algorithm coefficients are generally much smaller than coefficient values, except few cases where the differences are of the same order as the coefficient values.

To represent the contribution of all coefficients to the magnetic field we calculated the spatial power spectrum (with n up to a maximum degree $N_{\max} = 134$) (Lowes, 1974):

$$W_n = (n+1)\sum_{m=0}^{n}[(G_n^m)^2 + (H_n^m)^2] \qquad (3.8)$$

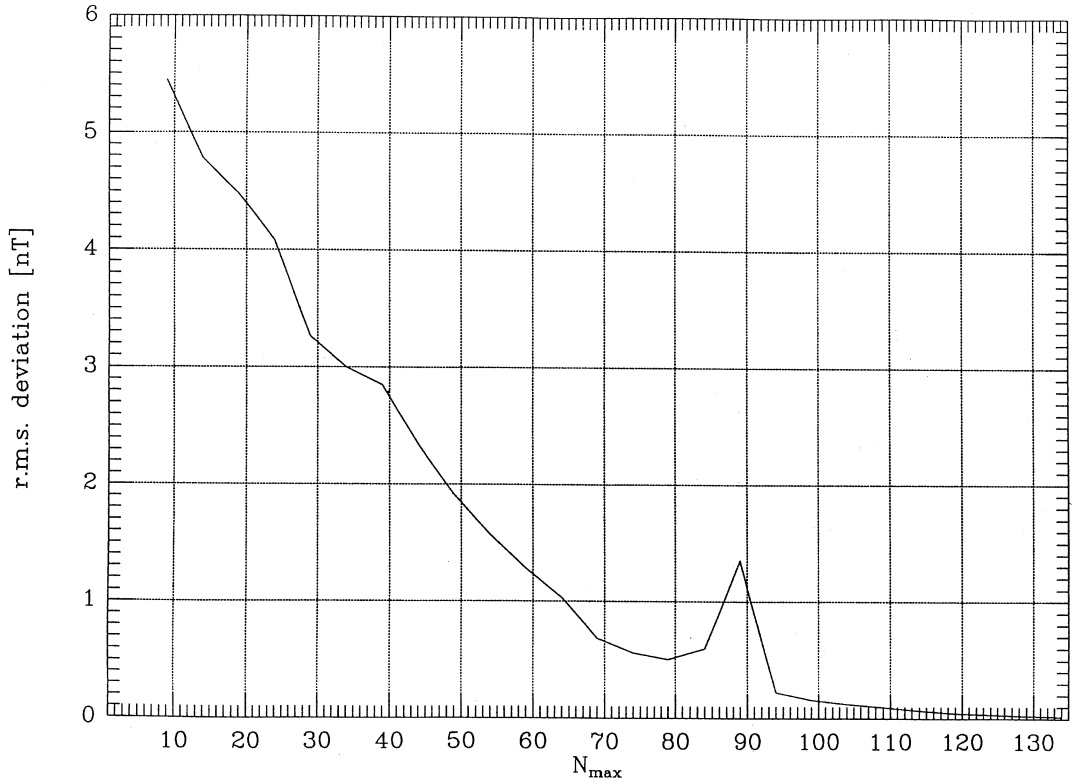

Fig. 8. The r.m.s. deviation between input field data and calculated field by the truncated spherical series depending on truncation level.

Figure 6 shows the spatial spectrum (in logarithmic scale) of the crustal field for two methods of SHC calculation (the dashed graphic is obtained with Gauss-Legendre quadrature and the solid graphic is obtained with Hurwitz method). Both graphics have the same pattern; the spectrum for Gauss-Legendre quadrature is a little higher than the spectrum for Hurwitz method. It seems that the contribution of higher harmonics increases getting a sharp maximum at about n=90. This is expected from our crustal model, because there must be an important harmonic with degree n=360°/4°=90, since 4° is the angular dimension of each crustal block (see also fig. 3). After such a maximum the increase of spectrum becomes smaller.

It can be shown that a model of N purely random radial dipoles at radial distance αa ($\alpha = r_i/a$, with r_i radial distance of dipoles and a the radius of reference sphere) has a spatial spectrum proportional to $Nn^2(n+1)\alpha^{2n}$ (Lowes, personal communications). We tested such a formula for our model of dipoles at depth 15 km and a=6371.2 km ($\alpha = 0.98195$). It would be expected the maximum of spectrum at about n=676. This case should not allow us to see this maximum. On the other hand if the radius of reference sphere of the spherical harmonic expansion of the magnetic potential is a=6371.2+450=6821.2, it would be expected the maximum at about n=20.

From the calculated spectrum of our crustal model field at reference a_1=6371.2 km, we

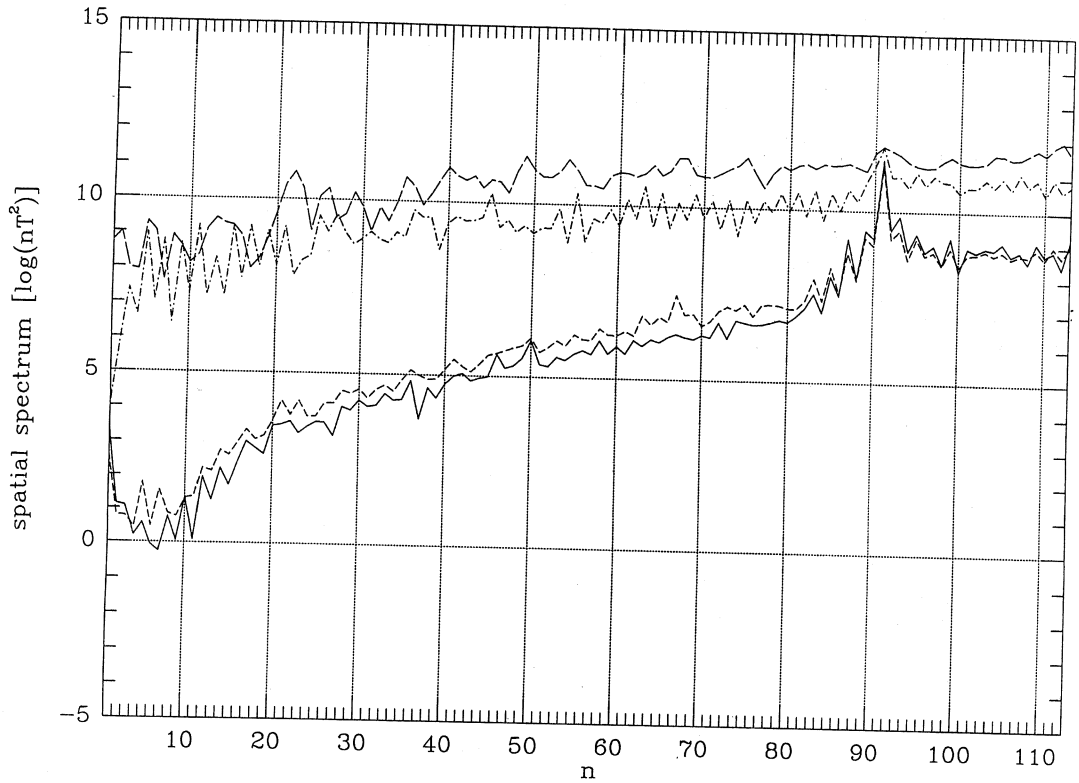

Fig. 9. Power spatial spectra obtained for series of data taken at different altitudes.

have calculated the corresponding spectrum at the reference a_2=6821.2 according to the formula (Meyer *et al.*, 1983):

$$W_n(a_2) = W_n(a_1) \cdot (a_1/a_2)^{2(n+2)} \qquad (3.9)$$

Such a spectrum is shown in fig. 7 (the dashed graphic is for Gauss-Legendre quadrature and the solid graphic is for Hurwitz method), where the maximum at about n=20 can be seen. This confirms that our crustal model is close to be a model of N purely random radial dipoles and the decrease of the spectrum the Earth's surface is expected to be at n higher than n=134.

We have recalculated the crustal field values in a meridian by the truncated spherical harmonic sum when the SHC are those calculated by Gauss-Legendre quadrature. Those values are compared with the modelled crustal field values at the same points. In fig. 8 is shown the r.m.s. deviation between the modelled crustal field values and the recalculated field values for different truncation (maximum degree N_{max}). It needs a high level of truncation (N_{max}>100) to get a reasonable deviation. There is amelioration during the increase of truncation level up to N_{max} = 80 and there is an aggravation around N_{max} = 90; after this, the deviation decreases with the increasing of truncation level. After including in the spherical harmonic sum the harmonics with degrees around n=90, we achieved the r.m.s. deviation one order smaller than the mean field value.

4. Conclusions

In the first part of the study we have brought out the advantages of Gauss- Legendre quadrature for the SHC calculation. Hence in all following calculations this algorithm was used.

We have tested the SHC calculation from the simulated data of crustal model field at different altitude h=0, 10, 100, 450 km and we noticed that the nearer the data are to the dipoles the greater the differences between the calculated SHC and true SHC. In order to reveal if there was a numerical instability we analysed the crustal model field adding to it a constant vertical field (field of a centred monopole) of 500 nT and we found the same values of coefficients. Then we thought that there was an «aliasing» effect. Plotting the values of the crustal model field along a meridian we found abrupt changes near the dipoles, which are not reflected in our data sampling. We tried a denser data grid and, as it can be shown (fig. 9), a smaller deviation from the true spectrum *i.e.* a smaller «aliasing» effect was found. In fig. 9 are shown the spectra for calculated SHC from the data at h=10 km of 115 200 grid points (dashed-pointed graphic) and of 76 800 grid points (the dashed-lined graphic), for calculated SHC from data at h=100 km of 76 800 grid points (dashed graphic) and for true SHC (solid graphic). As it is known the «aliasing» effect can be eliminated by low-pass filtering the original data; in practice this was made by upward continuing the field at h=100 km or at h=450 km.

Seeing the deviation between the modelled field and the recalculated field, we can conclude that for the SHA of a crustal field more than n=134 degree SHC computation is needed (being always under the Nyquist frequency).

Looking at the SHC values, we noticed that the greatest coefficient value is that of n=1, m=0 which belongs to the dipolar term. The reason could be that we have considered only induced magnetization from the core field, which is mostly dipolar.

In the well known procedure of separation the crust and core contribution to the internal geomagnetic field (Benton and Alldredge, 1987; Cain *et al.*, 1983; Lowes, 1974; Szeto and Cannon, 1985), (based on the fact that the spectrum of the whole internal field has two different slopes above and below degree 14: the low-degree part of the spectrum is assigned to the core and the remainder to the crust), the low degree harmonics of crustal field are included in the core contribution. Even the SHC of crustal origin are too much smaller than the SHC of core origin (in our crustal model the first coefficient is nearly 10^{-4} times smaller than the first coefficient of core field). We must keep in mind that in low degree and order harmonics of whole internal field a minor part of crustal contribution is hidden (Wonik, 1990).

Acknowledgements

The author undertook this work with the support of the «ICTP Program for Training and Research in Italian Laboratories, Trieste, Italy» at the Istituto Nazionale di Geofisica. The author is most grateful to Dr. A. Meloni and to the Unit of Geomagnetism (ING) for the friendly hospitality and help. He would like to thank especially Dr. F.J. Lowes and Dr. A. De Santis for scientific discussion and helpful suggestions.

REFERENCES

ABRAMOWITZ, N. and I.A. STEGUN (1972): *Handbook of Mathematical Functions* (Dover publications INC, New York).

ALLDREDGE, L.R. and K. KAWASAKI, (1981): Spherical harmonic analysis in the presence of high harmonics, *J. Geomagn. Geoelectr.*, **33**, 508-515.

BARRACLOUGH, D.R. (1987): International geomagnetic reference field: the fourth generation, *Phys. Earth Planet. Inter.*, **48**, 279-292.

BENTON, E.R. and L.R. ALLDREDGE (1987): On the interpretation of the geomagnetic energy spectrum, *Phys. Earth Planet. Inter.*, **48**, 265-278.

CAIN, J.C., B. HOLTER and D. SANDEE (1990): Numerical experiment in geomagnetic modeling, *J. Geomagn. Geoelectr.*, **42**, 973-987.

CAIN, J.C., ZH. WANG, D.R. SCHMITZ and J. MEYER

(1983): The geomagnetic spectrum for 1980 and core-crust separation, *Geophys. J.*, **97**, 443-447.

CAIN, J.C., ZH. WANG, C. KLUTH and D.R. SCHMITZ (1989): The derivation of a geomagnetic model to n=63, *Geophys. J.*, **97**, 431-441.

DE SANTIS, A. (1991): Translated origin spherical cap harmonic analysis, *Geophys. J. Int.*, **106**, 253-263.

HAINES, G.V. (1985): Spherical cap harmonic analysis, *J. Geophys. Res.*, **90**, (B3), 2583-2592.

HURWITZ, L. (1960): Eccentric dipoles and spherical harmonic analysis, *J. Geophys. Res.*, **65**, (8), 2555-2556.

KAWASAKI, K., S. MATSUSHITA and J.C. CAIN (1989): Least squares and integral methods of spherical harmonic analysis of the Sq-field, *Pure Appl. Geophys.*, **131**, 357-370.

LOWES, F.J. (1974): Spatial power spectrum of the main geomagnetic field and extrapolation to the core, *Geophys. J.R. Astron. Soc.*, **36**, 717-730.

MEYER, J., J.H. HUFEN, M. SIEBERT and A. HAHN (1983): Investigations of the internal geomagnetic field by means of a global model of the Earth's crust, *J. Geophys.*, **52**, 71-84.

PRESS, H.W., B.P. FLANNERY, S.A. TEUKOLSKY and W.H. VETTERLING (1987): *Numerical Recipes*, (Cambridge University Press).

QUINN, J.M. and G.A. BARRICK (1987): Spherical harmonic modelling of the geomagnetic field using the Fast Fourier transform, *Phys. Earth Planet. Inter.*, **48**, 206-220.

SCHMITZ, D.R. and J.C. CAIN (1983): Geomagnetic spherical harmonic analysis 1. Techniques, *J. Geophys. Res.*, **88**, (B2), 1222-1228.

SCHMITZ, D.R., J. MEYER and J.C. CAIN (1989): Modelling the Earth's geomagnetic field to high degree and order, *Geophys. J.*, **97**, 421-430.

SZETO, A.M.K. and W.H. CANNON (1985): On the core and crustal contribution to the geomagnetic field, *Geophys. J.R. Astron. Soc.*, **82**, 319-329.

WHALER, K.A. and D. GUBBINS (1981): Spherical harmonic analysis of the geomagnetic field: an example of a linear inverse problem, *Geophys. J.R. Astron. Soc.*, **65**, 645-693.

WONIK, T. (1990): Experience with the use of global reference field for compilation of aeromagnetic data for Europe, *J. Geomagn. Geoelectr.*, **42**, 1087-1097.

(received January 14, 1993;
accepted August 10, 1993)